Available online at www.sciencedirect.com

ScienceDirect

materialstoday: PROCEEDINGS

Materials Today: Proceedings 2 (2015) 3853 – 3863

The Selected Papers of 10th International Conference on Physics of Advanced Materials, ICPAM-10

Polymer Nanocomposites for Energy Storage Applications

Brian C. Riggs[a]*, Shiva Adireddy[a]*, Carolyn H. Rehm[a], Venkata S. Puli[a], Ravinder Elupula[b], Douglas B. Chrisey[a]

[a]Tulane University, Department of Physics and Engineering Physics, New Orleans, LA
[b]Tulane University, Department of Chemistry, New Orleans, LA

Abstract

To meet the rising need for on-demand electric energy, dielectric capacitors have been of increasing interest owing to their unique energy storage properties. The ability to deliver large amounts energy near instantaneously with a simple device that can last over millions of cycles is making dielectric capacitors one of the most attractive future options for large-scale electrical energy storage. The low gravimetric energy density, however, has prevented its widespread application in a wide range of fields including electric vehicles, and personal power technologies. Ceramic and polymer materials are being developed for energy storage, however, intrinsic limits on their dielectric properties (e.g., breakdown field and dielectric constant, respectively) prevents them from being used for high energy density applications. Because of this, composite systems of ceramics and polymers have been of increasing interest as they hold the potential for simultaneous improvement of both the dielectric constant and breakdown field leading to significant improvements in the energy storage potential. Herein we present new results and discuss the state of dielectric capacitor research including a discussion of the properties of interest. Recent developments in the field will be discussed including improvements in material properties, processing, and interface issues that arise when compositing materials as well as solutions to overcome these obstacles.

Selection and peer-review under responsibility of the conference committee of the 10th International Conference on Physics of Advanced Materials

Keywords: Energy storage; capacitors; dielectric properties; ink-jet printing; breakdown theory; polymers; nanocomposites; nanoparticles; thiol-click reactions

Corresponding Authors:
Brian C. Riggs; E-mail: briggs1@tulane.edu; Tel: +1-781-929-8793
Shiva Adireddy; E-mail: sadiredd@tulane.edu or shiva.adireddy@gmail.com; Tel: +1-504-810-0495

2214-7853
Selection and peer-review under responsibility of the conference committee of the 10th International Conference on Physics of Advanced Materials
doi:10.1016/j.matpr.2015.08.004

1. Introduction

1.1. Need for Dielectric Energy Storage

Ceramic capacitors are the most prevalent passive components in modern electronics. Exhibiting higher power densities than their energy storing alternatives, capacitors have gained attention for developing inexpensive and high performing energy storage devices [1]**.** Capacitance in multilayer ceramic capacitors has increased exponentially in recent years. With higher volumetric efficiency, and up to 1000 layers, maximum capacitance has been doubling every 13 to 14 months [2]**.** Unfortunately, capacitors still are not developed with high enough energy densities to keep up with advanced applications [3]**.**

Dielectric materials are predominantly used for short term charge storage.[4–6] Their ability to discharge large current densities over a short time intervals and increased lifetimes compared to batteries makes them potentially attractive for a wide range of applications including personal electronics and electric vehicles.[1] The energy stored within a dielectric is directly related to its dielectric properties such as its dielectric polarization, dielectric constant, conductivity, and breakdown strength. The energy density (E_d) of these prototype devices is the integral area of the polarization-electric field (P-E) and given by (1) and (2). The maximum energy storage per unit volume or dielectric energy density storage value is calculated using the volumetric energy equation for linear dielectrics (3). The energy storage density (E_d) is related to dielectric permittivity and the square of the breakdown voltage.

$$E_d = \int EdP \tag{1}$$

$$E_d = \frac{1}{2} \cdot \varepsilon_0 \cdot \varepsilon_r \cdot E_b^2 = \frac{1}{2} \cdot C \cdot V_m^2 \cdot \frac{1}{Ad} \tag{2}$$

where the applied electric field (E), polarization (P), breakdown strength (E_b) the permittivity ($\varepsilon = \varepsilon_r \, \varepsilon_0$), relative permittivity (ε_r), and the permittivity of free space ($\varepsilon_0 = 8.854 \times 10^{-14}$ F/cm). These material properties are of most interest when designing a dielectric capacitor for large scale energy storage

This paper will discuss the various concerns and factors involved with increasing the material properties stated in the equation above through polymer-ceramic nanocomposites. Fig. 1 shows schematically the intention behind combining a highly polarizable ferroelectric with a high linear dielectric strength. By doing this, the composite structure should have a balance of both properties and lead to an increase in energy storage. Before manufacturing and processing nanocomposites can be discussed, a quick overview of the material properties is necessary.

1.2. Dielectric and Breakdown Theory

As stated above, when designing a capacitive energy storage device the two properties of interest are dielectric constant and breakdown field. The dielectric constant of a material is a result of the reaction of permanent and induced dipoles in a material to an applied electric field.

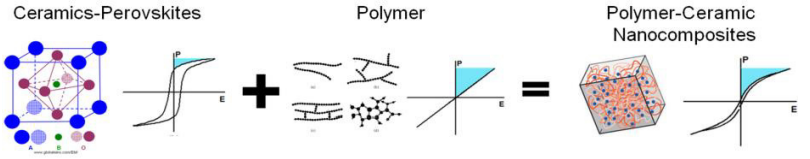

Fig. 1: Schematic of nanocomposites for energy storage

Under an applied field, induced dipoles create local internal fields, which counteract and reduce the applied field. Materials with high dielectric constants will have greater electric displacements at lower fields. This dielectric response

is present in a wide range of materials but most notably in ferroelectric perovskite ceramics and, to a lesser extent, ferroelectric polymers. The other property that determines energy storage, dielectric strength or breakdown field, determines the maximum field that can be applied to a material before failure occurs. A material is considered to have failed in an electric field when the behavior of the material switches from insulating to conducting. A material can fail in many ways including electronic, thermal, and electromechanical breakdown [7–20]. The greatest breakdown fields will occur in an electronic mode when a significant amount of electrons are excited from the valence to conduction band. However, flaws and defects within a material can significantly lower the theoretical breakdown strength by creating charge concentration areas or regions with lower intrinsic breakdown such as voids. Thermal breakdown occurs when the resistive heating exceeds that of convective cooling in a material. When the internal temperature of a material rises above a critical temperature, the sample will melt, degrade, or transform into a phase with a lower intrinsic breakdown strength. For practical applications, thermal breakdown is of most interest for polymer systems and will be discussed more in depth later. Electromechanical failure is caused by the weak attraction of the cathode and anode causing compressive stress on the sample. If a high enough field is applied to induce a stress upon the material beyond its yield stress, the sample will fracture. For soft samples, the induced compressive stress will reduce the thickness of a sample increasing the local field, allowing another mechanism to cause breakdown. With these modes in mind, materials can be designed in order to increase the theoretical breakdown strength.

2. Materials for Energy Storage Applications

2.1. Ceramics and Methods of Ceramic Nanoparticle Synthesis

Dielectric ceramics have been of significant interest due to their large dielectric constants [21–31]. The largest drawback is their reduced breakdown strength, which is primarily due to processing flaws. Eliminating these flaws to increase the breakdown strength for device applications is arduous and costly. There has been significant work reducing the defects and porosity within bulk ceramics through high temperature, high pressure treatments, producing thin films through sputtering or pulsed laser deposition, or forming nanoparticle (NP) films through sol-gel processing [32–36], but the cost/kWh of the formed devices does not justify using these processing technique for large scale applications. An alternative approach involves compositing the dielectric powder with materials that intrinsically are considered "defect free" and form hermetically sealing interfaces, such as glass [26,37–47] and polymers [15,28,48–55]. This method is especially attractive due to the low processing temperatures, ease of processing, and significant improvements in performance. One major concern when compositing is the interface interaction between the dielectric NP and high breakdown matrix. An abrupt interface containing dangling bonds will cause interfacial flaws that will lower the dielectric strength below intrinsic values. A significant amount of work has been dedicated to developing a dielectric NP [25,56–60], high breakdown matrix (glass or polymer), and interface necessary to prevent a decrease in performance. Furthermore, precise control of stoichiometry, size, shape, and distribution of these ceramic NPs is crucial for a successful nanocomposite.

Morphology-controlled colloidal nanocrystals have been applied in many fields, including electronics, optics, mechanics, magnetics, and catalysis. Synthetic protocol that enables large-scale production of morphology-controlled nanocrystals is, therefore, of key general importance. In order to create these nanocomposites, several methods of NP synthesis have been investigated. Current synthetic strategies include sol-gel, combustion, co-precipitation [61], as well as organic solution-phase synthesis, thermolysis of organometallic precursors, hydrothermal, microwave hydrothermal methods, and biomimetic and dendrimer templating.

Traditional ceramic methods involve grinding portions of the desired elements and heating them together at extreme temperatures (>1000°C). This method has excellent control of stoichiometry and creates a very crystalline product. However, there is no particle size control and cycles of heating and grinding are lengthy [63–65]. Another method, the sol-gel method, involves mixing soluble metal reagents into a colloidal solution to form an amorphous precipitate before performing calcination to remove by-products. While this process creates a homogenous product, the gel often leaves behind impurities and particle size control is very difficult [63,66,67]. The molten salt method uses a molten liquid reaction medium for better diffusion. This method also produces a very homogenous product, and burns off organic components in a single step. However, size control is a concern here as well [64,68,69]. Often, however, most

of these procedures require stringent experimental conditions, are difficult to generalize, or necessitate tedious multistep reactions and purification.

Our research group has used a general strategy for crafting a variety of ferroelectric and dielectric nanocrystals with precisely controlled dimensions and chemical compositions by using surfactant-assisted solvothermal method [56,70]. Our approach enables the facile synthesis of organic solvent-soluble colloidal nanocrystals with desired composition. Recently, we demonstrated the generality of our approach by describing, as examples, the synthesis of ferroelectric, semiconductor, and magnetic nanocrystals and their composites [71–73]. The solvothermal method offers an attractive means by which to synthesize monodispersed nanocrystals because of its ability to direct the aggregation of inorganic materials in well-defined volumes. The solvothermal method involves exposing a solution in sealed stainless steel pressure reaction vessel to temperatures above the boiling point of its solvents [74,75]. NP growth process in surfactant-assisted solvothermal method depend heavily on temperature, ingenious pressure, solvent characteristics and pH [64,66].

2.2. Polymer Dielectrics

Polymer dielectrics have been sought after in the microelectronics industry for their high manufacturability and low dielectric constants, making them suitable candidates for transistor gate dielectrics [76–79]. Their low leakage currents allow for nanometer thin layers to be utilized without loss of functionality, which contributes to the miniaturization of devices. While the low loss and low dielectric constant is attractive for transistor applications, a higher dielectric constant is necessary for energy storage applications. This issue prompted a significant amount of research over the past 50 years on ferroelectric polymers, which have significantly higher dielectric constants compared to dielectric polymers.

While the dielectric constant in ceramics arises predominantly from the asymmetrical central cation shift, a form of ionic polarization, polymers have many sources for their dielectric constant. The three main contributions in polymers are orientation, ionic, and electronic. Orientation polarization arises from increased chain mobility, which allows permanent dipoles to align themselves with the electric field. This is relatively rare in practical polymers as the mobility necessary for orientation polarization to be active leads to viscous polymer fluids rather than a solid film. Ionic/atomic polarizations arise when an entire atom shifts within the applied field such as in perovskite ceramics. PVDF, polyvinylidene fluoride, is the most notable example as the negatively charged fluorine and positively charged hydrogen stretch in the direction of the field. When PVDF is in the beta phase, the dipole moments are aligned so that there is a net electric field (Fig.2).

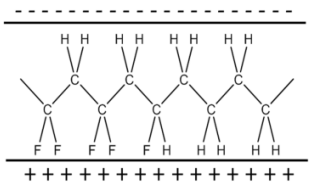

Fig. 2: Schematic of the ferroelectric phase of PVDF. Notice the separation of hydrogen and fluorine creates discreet electronic domains

These discreet domains allow for out of plane polarization when a field is applied contributing to a higher dielectric constant (~14). The creation of discreet charge domains within a polymer is one method to design high dielectric constant polymer systems. Another method is to create dipole interactions between chains of the polymer. Burlingame et al.[80] demonstrated how the dielectric constant of polyureas could be increased by substituting the carbonyl for sulfur, creating polythiouruea, increasing the strength of the interaction between inter-chain hydrogen and sulfur, and therefore the dielectric constant. The creation of stronger local internal fields, albeit at a moderate concentration (20 mol%), is enough to shift the dielectric constant from 4.2 to 4.5. Although electronic polarization is often discounted in ceramics due to the relatively weak response, in polymers it plays a much more significant role. Electronic polarization is utilized by including chemical groups that have highly reactive electron clouds. Although non-polar,

aromatic rings are easily polarized when exposed to an out-of-plane field[81]. The LUMO3σ* cloud responds strongly to an applied field. The inclusion of aromatic rings has been shown to increase the dielectric constant. Although the contribution from electronic polarization is small compared to other modes, the dominance of electronic polarization allows for frequency independence into the GHz range allowing for broader applications.

As discussed previously, the main reason for using polymeric matrices is their high breakdown strength. Although there are multiple modes of failure for polymer materials, thermal breakdown is the primary mode. This occurs when the resistive heating due to the leakage current raises the internal temperature of a material beyond a critical point at which point the material melts, changes to a phase with a lower breakdown strength, or decomposes. A simple balance of the heat generated from the induced current and the heat lost from convection over the material yields (3) in which the conductivity as a function of temperature, $\sigma(T)$, the critical temperature, T_c, and the areal thermal conductivity, γ, are material properties. V_{app} is the applied voltage, d is the film thickness and T_o is the temperature of the environment. Figure 3 plots (3), varying one material property while holding the others constant, to demonstrate the significance of each property. Although electrical and thermal conductivity will have the same degree of effect on breakdown strength, the change in electrical conductivity is much more likely to extend over several orders of magnitude, while the change in conductivity only extends over one. Because of this, electrical conductivity should be the largest concern when designing a material. Decreasing the degree of crystallinity or introducing dipole trap features that will reduce the overall kinetic energy of electrons, ultimately reducing the possibility for breakdown, can achieve this.

$$\frac{\sigma(T)\cdot V_{app}^2}{2d} = \gamma\left(T_c - T_0\right) \tag{3}$$

The advantages of using a polymer for energy storage application are improved processing and properties. Thin films of polymer materials can be cast in atmospheric conditions and can be exposed to minimal heat treatment (maximum of 300 °C) for curing processes. Some polymer systems, such as thiol click or acrylate monomers, can be cured using conventional or high-powered UV lamp systems. These are especially attractive due to the high wall-plug efficiency, rapid production rate, and the precedent of use in energy and electronic industries, compared to conventional furnaces necessary for ceramic processing[76,77,82–85]. Due to the quadratic relationship between breakdown and energy storage, obtaining a high breakdown field can be considered more important than obtaining a high dielectric constant. From this perspective, neat polymer dielectric capacitors[80,86] can obtain energy densities over 15 J/cm^3 compared to bulk ceramics[87–90], 3 J/cm^3. The increase in breakdown field is the largest advantage that polymers have over other materials for capacitor applications. However, their low dielectric constant (5-14) significantly limits their potential for applications in low field storage applications. However, the dielectric constant can be improved by compositing the polymer with high dielectric constant perovskite ceramics.

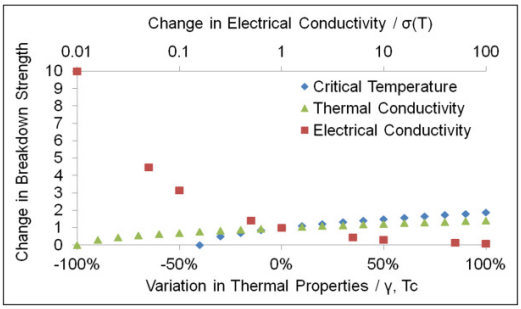

Fig. 3: The change in breakdown strength with variation of different material properties.

3. Ceramic-Polymer Nanocomposites for Increased Energy Storage

Studies are turning towards dielectric polymer nanocomposites in an attempt to develop higher energy densities. A

material's energy density is dictated by its relative dielectric permittivity and electric breakdown strength. Ceramic materials exhibit large dielectric permittivity but they generally have low breakdown strengths. Polymers have much higher breakdown strengths (>500 MV/m) but their dielectric permittivities are too low (>3) to provide significant energy densities [91–93]. Ferroelectric ceramics with large dielectric permittivity have successfully been incorporated into polymer matrixes, increasing their dielectric permittivity. Wang and Zhu increased a polyimide's dielectric permittivity to 49 at 100 Hz, 14 times which of the polyimide alone, when calcium copper titanate was added [91]. Methods of dispersion are being investigated as well as the effect of the shape of the NPs. Wang and Zhu also have added conductive fillers to their composites and found the dielectric constant of the polymer matrix has increased up to hundreds of times. However, the addition of the conductor also increases the dielectric loss [91].

3.1. Nanocomposite fabrication methods

Once NPs with the desired characteristics are created, they must be assembled into useful structures. Conventional methods of capacitor production involve thick wet film processing and are unable to produce capacitors any thinner than ~ 1.0 μm [2]. Multiple alternative methods of assembly, referred to as solid freeform fabrication, have been investigated using layered deposition of colloidal inks to create thin films. Techniques include hot-melt printing, micropen, and robotic deposition. One of the most established technologies in solid freeform fabrication is ink-jet printing. Mastering ink-jet printing of nanocomposites would enable the production of a wide range of precise configurations and structures, which would not only enhance energy storage in current applications but serve as a building block for new applications as well [94–96].

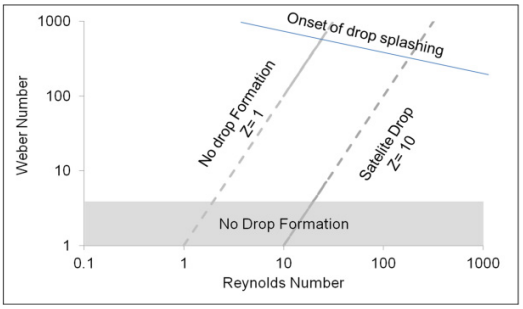

Figure 4: Plot of Reynolds number vs the square root of the Weber number. The interior region represents the fluid properties that will print without significant complications.

$$Z = \frac{\mathrm{Re}}{\sqrt{We}} = \frac{(\gamma \cdot \rho \cdot a)^{1/2}}{\eta} \tag{4}$$

As for any of the printing techniques, particular fluid dynamics are favourable. More specifically when the Z factor (4) has a value between 1 and 10, shown graphically in Figure 4, where Re is the Reynolds number, We is the Weber number, ρ is the ink density, η is the viscosity, γ is the surface tension, and a is the characteristic length, desirable drops are formed. When $\mathrm{Re}/\sqrt{We}$ values are not between 1 and 10, excess satellite droplets can form, print head nozzles can clog, or other undesirable printing defects can occur. Another aspect that must be taken into account is the rate at which the inks dry. Finding the appropriate rate is imperative, as the print head can clog if the solvents evaporate too quickly. If the rate is too slow, the inks spread uncontrollably. The size of the NPs suspended in the ink can also affect the efficacy of the printing. Particles should be less than a 100^{th} of the size of the print nozzle and should have narrow size distribution. These specifications are possible by the size control of the various wet-chemical methods such as solvothermal and thermolysis. By continuing to investigate ink formulation, ideal

fluid dynamics for ink-jet printing can be produced [94,97–100].

Fig. 5: Printed, flexible capacitor layers for energy storage applications

Once nanocomposite structures have been deposited via ink jet printing, photonic curing can be used to sinter. Using a flash lamp, films can be cured to high temperatures while keeping the substrate at a low temperature. The process is also much more efficient than traditional sintering methods [86,101,102]. This ink-jet printing process provides a method of freeform fabrication that is inexpensive, low waste, and low temperature, while also having the ability to create flexible electronic components. Success in freeform fabrication can lead to efficient production of dielectric polymer nanocomposite films able to be used in various applications including but not limited to mobile electronic devices, hybrid electric vehicles, and other electric power systems [94,103].

Recently, Riggs et al. have combined these processes to rapidly produce capacitor devices on the lab scale with a high breakdown polymer system [86]. The monomer ink incorporated several cross-linking units as well as a high percentage of aromatics in order to increase the dielectric constant and the thermal stability. Long aromatic chains formed amorphous regions, which decreased the conductivity, allowing for greater fields to be applied before the thermal breakdown sets in. By curing at high fluences (5 J/cm^2), thick films of the material could be cured within seconds to form mechanically and chemically stable films. These films, shown in Fig. 5, could reach energy densities of 32 J/cm^3 with a production rate easily scalable to commercial standards.

3.2. Predicting Composite Properties

Like most phenomena, dielectric properties are relatively simple to explain in bulk but become more complex in a multi-material system. Most dielectric responses are a bulk property, which relies on crystalline regions for self-polarization. The interactions between materials provide synergetic effects that shift the composite dielectric constant away from a simple mixing rule. The standard mixing rule used, follows a logarithmic rule of mixing (5)**Error! Reference source not found.**, where the logarithm of the dielectric constant of the composite (ε_c) equals the summation of the volume fraction of the components (V_n) times the logarithm of their dielectric constants (ε_n). This has been most often applied when discussing ceramic-polymer composites because the approximation is normally "good enough," but at the dilute volume fractions, the model breaks down.

$$\log \varepsilon_c = V_1 \cdot \log \varepsilon_1 + V_2 \cdot \log \varepsilon_2 \tag{5}$$

The logarithmic mixing rule is actually a special solution for the exponential mixing rule (6)**Error! Reference source not found.** where the exponent k = 0. Formerly, the parameter *k* is fit to the data through a least mean square linear regression. However, the extreme bounds of 1 and -1 can be visualized with a series or parallel circuit of capacitors. Other evaluations for k have been developed that rely on empirical results and finite element analysis for their derivation [104–106]. In general, the exponential models assume there is no interaction between the matrix and the filler material; the composite property will be some addition of the two components.

Effective medium theory assumes that a mixture of one dielectric constant surrounds each particle. This has a greater similarity to a bulk treatment as it recognizes the effects of the bulk surrounding material on a particle. After simplifying for spherical particles, (7), known as the Bruggeman symmetrical medium equation, can be used to approximate a composite dielectric constant [104,107]. The exponent *k* is determined by the type of mixture, i.e., *k* =

-1 for a parallel mixing model, k = 1 for a serial mixing model, k = 1/3 for a randomly distributed model. The Bruggeman equation assumes that the filler and matrix material are randomly distributed and have similar morphologies.

$$\varepsilon_c^k = V_1 \cdot \varepsilon_1^k + V_2 \cdot \varepsilon_{21}^k \tag{6}$$

$$V_1 \cdot \frac{\varepsilon_1 - \varepsilon_c}{\varepsilon_1 - 2\varepsilon_c} + V_2 \cdot \frac{\varepsilon_2 - \varepsilon_c}{\varepsilon_{21} - 2\varepsilon_c} = 0 \tag{7}$$

Although it could be argued that the breakdown field is of more importance than the dielectric constant due to the quadratic relation with energy storage, there are no mixing rules or approximations for dielectric strength. This is because breakdown phenomenon is not a bulk phenomenon but is a failure phenomenon caused by the defects that are introduced into the system by adding a ceramic filler. As most of these defects are due to the interface of the particle and polymer, a surface area mixing-rule would be more appropriate. However, little work has been done on modelling the relation between particle loading and breakdown strength. Any work that has been done has been empirical fitting of experimental data.

There are two major concerns when working with composite systems: the solubility of the NP in the polymer ink and the state of the interface after curing. The solubility of the NP obviously affects the printing and deposition capabilities. If the goal is inkjet printing, such in Ramakrishnan et al. [108], then a critical size and dispersion are necessary for particles to reliably pass through the nozzle. A poor dispersion will lead to particle aggregation that creates micron scale regions of "bulk" ceramic that will have the defects and voids that cause low breakdown. A poor dispersion will also result in a heterogeneous material with multiple phases, each with their own breakdown and dielectric properties. This heterogeneity greatly increases the variability in energy storage properties especially the shape parameter of the Weibull distribution, which relates to failure reliability for breakdown statistics. Once a material is cured, there is concern over the interaction between the dielectric NP and the polymer matrix. Ideally, there will be no change in the breakdown strength and an increase in the dielectric constant following closely to the logarithmic rule of mixing. However, it has been found that this is not that case, as dramatic decreases in breakdown strength have been reported. This is attributed to an incoherent interface between the NP and matrix. This interface acts as a void that has significantly lower breakdown strength. In order to solve this problem, the interface between particle and matrix should be controlled so that there is an attractive component. This benefit will be two-fold as to increase the solubility and the favorable interaction, leading to increased performance.

3.3. Recent Work in Nanocomposites

Dielectric polymer nanocomposites created by incorporating inorganic NPs into polymer matrices show promising energy storing properties, which would make for higher-performance capacitors. Recently, our group has explored the energy storage capability of polyvinylidene fluoride (PVDF)-based composites with variety of NPs including $BaTiO_3$, $Ba_{1-x}Ca_xTiO_3$ (X=0.3±0.05) [BCT], $BaZr_{1-x}Ti_xO_3$ (X=0.2±0.05) [BZT], and $Ba_{0.5}Sr_{0.5}TiO_3$ [BST] [109,110]. Colloidal NPs were initially prepared in high yield by a solvothermal method and used as fillers in PVDF polymer matrix. The unique dielectric-polymer films show enhanced dielectric constants, enhanced electrical breakdown strengths, and enhanced dielectric energy densities (Table 1). The matrices exhibit higher dielectric permittivities than those of the polymer alone as well as higher breakdown strengths than the ceramic materials. These nanocomposites materials also allow for more versatility than traditional ceramics used in capacitors as they are lighter in weight than ceramics alone and their flexibility allows them to be molded within electronics [111,112].

In general, NPs tend not to disperse homogenously in polymers. The inconsistency has a detrimental effect on the dielectric and breakdown properties, thus methods of proper dispersion have been investigated. Surface functionalization of the NPs allows for much more uniformity in composition as well as higher breakdown strength of the composite. For example, when Yu et al. modified $BaTiO_3$ with Polyvinylprroolidone (PVP), a more homogenous product was created with an increased dielectric permittivity of 77 at 1kHz, 28% higher than untreated $BaTiO_3$ [14].

Gao et al. has also modified nanomaterials to investigate interface properties. $BaTiO_3$/polyvinylidene fluoride nanocomposites were modified with DN-101. The polarization response of the material was improved by 18% to 240 MV/m and the dielectric breakdown strength from 240 MV/m to 260 MV/m. The result was an increase of 6.5 to 9.01 J/cm^3 in its energy density [113].

Table 1: Summary of properties of nanocomposite films with ceramic NP filler embedded in PVDF matrix [11, 12]

	E_c 1 kHz	E_b [MV/cm]	Tan δ	E_d [Jcm^{-3}]	Size of NPs [nm]	Filler loading (vol %)	Film Thickness [μm]
PVDF-BTO	15	2.25	<0.1	3.24	~10	18	~45
PVDF-BCT	35	1.75	<0.1	4.72	~15	18	~45
PVDF-BZT	28	2.5	<0.1	7.74	~8	18	~10

The most recent work has focused on modified the interface between particle and matrix in order to reduce the loss in breakdown strength due to the charge concentration and low breakdown interfaces [48,114]. In general the goal is to form a bond between the particle and the polymer as to eliminate the abrupt transition from polymer to ceramic. Zhou et al. [48] have approached the problem by introducing hydroxyl groups to the surface of barium titanate. When mixed with PVDF, the fluorine forms weak hydrogen bonds with the hydroxyl groups, allowing a greater volume percent to be mixed in and an increase of 17% in the breakdown field at 30 volume percent of dielectric. This is attributed to the reduction in voids at the interface, along with local diminishing of the applied electric field around the high dielectric constant filler. Another method of increasing the interaction between the particle and matrix is to graft the matrix material of interest direction onto the NP [91]. Li et al. demonstrated this by growing long, 240 kDa, PVDF co-polymer chains onto TiO_2 NPs. These particles could then be easily dispersed into a polymer matrix and cast into thin films [60]. These materials have shown only minor decreases in breakdown field but increases in dielectric constant consistent with the logarithmic rule of mixing. This has lead to an overall doubling of the energy storage capabilities (from 3.25 to ~7.0 J/cm^3) with 50% loading. A final method is the direct binding of the NP into a PVDF matrix. Dou et al. [55] showed that ferroelectric NPs could be functionalized with a titanate coupler agent (NDZ101) that has a functional allyl that could react with a PVDF co-polymer, increasing the strength of the binding between the particle and the matrix and improving the breakdown up until a critical loading.

4. Conclusions and Summary

Dielectric capacitors for energy storage would be a large advancement for many applications including personal power, electric vehicles, defence technology, and grid scale load levelling. Their long lifetime and high power densities make them ideal candidates for applications beyond microelectronic. However, the low energy density they provide, currently eliminates them from expanding into greater markets. Both conventional ferroelectric ceramics and insulation polymers have been of interest to increase the energy storage capabilities by maximizing the dielectric constant and breakdown field respectively, however sacrifice other properties. In the past ten years, a new line of materials, nanocomposites, have become of interest due to the possibility of increasing both properties. The added benefits of manufacturing ease and low materials cost make polymer-ceramic nanocomposites especially interesting. Energy densities up to 20 J/cm^3 have been achieved by designing polymers to have greater breakdown fields, and engineering the interface between the two materials in order to eliminate any defects through careful controlling of NP size, shape, and stoichiometry. Future work will focus on studying the interface at a fundamental level to better understand how future improvements can be made.

5. References

[1] G.H. Haertling, J. Am. Ceram. Soc. 82 (1999) 797..
[2] M.J. Pan, C.A. Randall, IEEE Electr. Insul. Mag. 26 (2010) 44.
[3] Q. Wang, L. Zhu, J. Polym. Sci. Part B-Polymer Phys. 49 (2011) 1421.
[4] C.W. Beier, J.M. Sanders, Brutchey, J. Phys. Chem. C 117 (2013) 6958.
[5] Y.R. Lin, H.A. Sodano, J. Appl. Phys. 106 (2009).
[6] V.K. Thakur, E.J. Tan, M.F. Lin, P.S. Lee, Polym. Chem. 2 (2011) 2000.
[7] N. Zebouchi, D. Malec, J. Appl. Phys. 83 (1998) 6190.
[8] Z.L. Bilr, L.I.N.C. I, (1997).
[9] J.W. McPherson, R.B. Khamankar, A. Shanware, J. Appl. Phys. 88 (2000).
[10] J. Huang, Y. Zhang, T. Ma, H. Li, L. Zhang, Appl. Phys. Lett. 96 (2010) 042902.
[11] M. Meunier, N. Quirke, J. Chem. Phys. 113 (2000) 369.
[12] A.D. Milliken, A.J. Bell, J.F. Scott, Appl. Phys. Lett. 90 (2007) 112910.
[13] Y. Wang, X. Zhou, M. Lin, Q.M. Zhang, Appl. Phys. Lett. 94 (2009) 202905.
[14] M. Masuduzzaman, S. Xie, J. Chung, D. Varghese, J. Rodriguez, S. Krishnan, M. Ashraful Alam, Appl. Phys. Lett. 101 (2012) 153511.
[15] P. Barber, S. Balasubramanian, Y. Anguchamy, S. Gong, A. Wibowo, H. Gao, H.J. Ploehn, H.-C. zur Loye, Polymer Composite and Nanocomposite Dielectric Materials for Pulse Power Energy Storage, 2009.
[16] H.D. Chen, K.R. Udayakumar, Integr. Ferroelectr. 15 (1997) 89.
[17] Y. Wang, X. Zhou, Q. Chen, B. Chu, Q. Zhang, IEEE Trans. Dielectr. Electr. Insul. 17 (2010) 1036.
[18] M. Meunier, N. Quirke, a. Aslanides, J. Chem. Phys. 115 (2001) 2876.
[19] M. Ieda, IEEE Trans. Electr. Insul. E1-15 (1980) 206.
[20] L.A. Dissado, J.C. Fothergill, Electrical Degradation and Breakdown in Polymers, 2008.
[21] H.-I. Hsiang, L.-T. Mei, W.-C. Liao, F.-S. Yen, J. Am. Ceram. Soc. 1717 (2010) no.
[22] D.Y. Kaufman, S.K. Streiffer, J. Zebrowskif, T. Pennsylvania, (1999).
[23] D.-Y. Gui, H. Liu, H. Hao, Y. Sun, M. Cao, Z.-Y. Yu, ChemSusChem 4 (2011) 1470.
[24] M. Cannon, (2011) 1.
[25] A.K. Nikumbh, P. V. Adhyapak, Particuology (2012).
[26] J. Du, B. Jones, M. Lanagan, Mater. Lett. 59 (2005) 2821.
[27] B. Ma, D.-K. Kwon, M. Narayanan, U. (Balu) Balachandran, Mater. Lett. 62 (2008) 3573.
[28] J. Lim, J. Kim, Y.J. Yoon, H. Kim, H.G. Yoon, S.-N. Lee, J. Kim, Int. J. Appl. Ceram. Technol. 9 (2012) 199.
[29] S.E. Company, N. Adams, 7 (1972) 339.
[30] J. Sigman, G.L. Brennecka, P.G. Clem, B. a. Tuttle, J. Am. Ceram. Soc. 91 (2008) 1851.
[31] R.A. Islam, S. Priya, Appl. Phys. Lett. 88 (2006) 032903.
[32] C. Elissalde, M. Maglione, C. Estournès, J. Am. Ceram. Soc. 90 (2007) 973.
[33] Z. Zhao, V. Buscaglia, M. Viviani, M. Buscaglia, L. Mitoseriu, A. Testino, M. Nygren, M. Johnsson, P. Nanni, Phys. Rev. B 70 (2004) 1.
[34] C.-F. Chen, D.W. Reagor, S.J. Russell, Q.R. Marksteiner, L.M. Earley, D. a. Dalmas, H.M. Volz, D.R. Guidry, P. a. Papin, P. Yang, J. Am. Ceram. Soc. 94 (2011) 3727.
[35] L. Curecheriu, M.T. Buscaglia, V. Buscaglia, Z. Zhao, L. Mitoseriu, Appl. Phys. Lett. 97 (2010) 242909.
[36] C.N. George, J.K. Thomas, H.P. Kumar, M.K. Suresh, V.R. Kumar, P.R.S. Wariar, R. Jose, J. Koshy, Mater. Charact. 60 (2009) 322.
[37] X. Wei, H. Yan, T. Wang, Q. Hu, G. Viola, S. Grasso, Q. Jiang, L. Jin, Z. Xu, M.J. Reece, J. Appl. Phys. 113 (2013) 024103.
[38] S.-F. Wang, Y.-R. Wang, Y.-F. Hsu, C.-C. Chiang, J. Alloys Compd. 498 (2010) 211.
[39] Y. Zhou, Q. Zhang, J. Luo, Q. Tang, J. Du, Scr. Mater. 65 (2011) 296.
[40] S.-G. Kim, J.-S. Park, J.-S. An, K. Sun Hong, H. Shin, H. Kim, J. Am. Ceram. Soc. 89 (2006) 902.
[41] D.-X. Zhou, R.-G. Sun, S.-P. Gong, Y.-X. Hu, Ceram. Int. 37 (2011) 2377.
[42] K. Kageyama, J. Takahashi, J. Am. Ceram. Soc. 87 (2004) 1602.
[43] Y. Zhang, J. Huang, T. Ma, X. Wang, C. Deng, X. Dai, J. Am. Ceram. Soc. 94 (2011) 1805.
[44] X. Su, M. Tomozawa, J.K. Nelson, D.B. Chrisey, J. Mater. Sci. Mater. Electron. (2013) 3.
[45] H. Jiang, J. Zhai, X. Chou, X. Yao, Ferroelectrics 403 (2010) 11.
[46] G. Senthil Murugan, K. Varma, Solid State Ionics 139 (2001) 105.
[47] C. Busta, On the Dielectric Properties of 0.3BaO-0.45B2O3-0.25ZnO and 0.5PbO-0.4 SiO2-0.1Al2o3 Glass in Bulk and Film Forms, 2011.
[48] T. Zhou, J.-W. Zha, R.-Y. Cui, B.-H. Fan, J.-K. Yuan, Z.-M. Dang, ACS Appl. Mater. Interfaces 3 (2011) 2184.
[49] P. Barber, P.J. Pellechia, H.J. Ploehn, H.-C. zur Loye, ACS Appl. Mater. Interfaces 2 (2010) 2553.
[50] R. Popielarz, C.K. Chiang, R. Nozaki, J. Obrzut, Macromolecules 34 (2001) 5910.
[51] R. Popielarz, C.K. Chiang, Mater. Sci. Eng. B 139 (2007) 48.
[52] Y. Rao, C.P. Wong, J. Appl. Polym. Sci. 92 (2004) 2228.
[53] M. Arbatti, X. Shan, Z.-Y. Cheng, Adv. Mater. 19 (2007) 1369.
[54] Y. Bai, Z.-Y. Cheng, V. Bharti, H.S. Xu, Q.M. Zhang, Appl. Phys. Lett. 76 (2000) 3804.
[55] X. Dou, X. Liu, Y. Zhang, H. Feng, J.-F. Chen, S. Du, Appl. Phys. Lett. 95 (2009) 132904.
[56] S. Adireddy, C. Lin, B. Cao, W. Zhou, G. Caruntu, Chem. Mater. 22 (2010) 1946.

[57] Y. Zhang, X. Wang, J.-Y. Kim, Z. Tian, J. Fang, K.-H. Hur, L. Li, J. Am. Ceram. Soc. 95 (2012) 1628.
[58] H.M. Jung, J.-H. Kang, S.Y. Yang, J.C. Won, Y.S. Kim, Chem. Mater. 22 (2010) 450.
[59] S. Aoyagi, Y. Kuroiwa, A. Sawada, H. Kawaji, T. Atake, J. Therm. Anal. Calorim. 81 (2005) 627.
[60] J. Li, S. Il Seok, B. Chu, F. Dogan, Q. Zhang, Q. Wang, Adv. Mater. 21 (2009) 217.[61] X. Li, W. Shih, J. Am. Ceram. Soc. 80 (1997) 2844.
[62] R. Asiaie, W.D. Zhu, S.A. Akbar, P.K. Dutta, Chem. Mater. 8 (1996) 226.
[63] D. Astruc, F. Lu, J.R. Aranzaes, Angew. Chemie-International Ed. 44 (2005) 7852.
[64] R.I. Walton, Chem. Soc. Rev. 31 (2002) 230.
[65] X. Wei, G. Xu, Z.H. Ren, Y.G. Wang, G. Shen, G.R. Han, J. Am. Ceram. Soc. 91 (2008) 315.
[66] S.H. Yu, J. Ceram. Soc. Japan 109 (2001) S65.
[67] K. Byrappa, J. Ceram. Soc. Japan 117 (2009) 236.
[68] M. Zawadzki, J. Alloys Compd. 454 (2008) 347.
[69] P.H. Mutin, A. Vioux, Chem. Mater. 21 (2009) 582.
[70] S. Adireddy, C.E. Carbo, T. Rostamzadeh, J.M. Vargas, L. Spinu, J.B. Wiley, Angew. Chemie-International Ed. 53 (2014) 4614.
[71] S. Adireddy, C.E. Carbo, Y. Yao, J.M. Vargas, L. Spinu, J.B. Wiley, Chem. Mater. 25 (2013) 3902.
[72] S. Adireddy, Y. Yao, J. He, J.B. Wiley, Mater. Res. Bull. 48 (2013) 3236.
[73] D. Mohanty, G.S. Chaubey, A. Yourdkhani, S. Adireddy, G. Caruntu, J.B. Wiley, Rsc Adv. 2 (2012) 1913.
[74] U.K. Gautam, M. Rajamathi, F. Meldrum, P.E.D. Morgan, R. Seshadri, Chem. Commun. (2001) 629.
[75] S. Thimmaiah, M. Rajamathi, N. Singh, P. Bera, F. Meldrum, N. Chandrasekhar, R. Seshadri, J. Mater. Chem. 11 (2001) 3215.
[76] C. Wang, W.-Y. Lee, R. Nakajima, J. Mei, D.H. Kim, Z. Bao, Chem. Mater. 25 (2013) 4806.
[77] J.M. Ko, Y.H. Kang, C. Lee, S.Y. Cho, J. Mater. Chem. C 1 (2013) 3091.
[78] W. Clemens, W. Fix, J. Ficker, a. Knobloch, a. Ullmann, J. Mater. Res. 19 (2011) 1963.
[79] G. Maier, D.- Garching, 26 (2001).
[80] Q. Burlingame, S. Wu, M. Lin, Q.M. Zhang, Adv. Energy Mater. 3 (2013) 1051.
[81] W.Y. Kim, Y.C. Choi, K.S. Kim, J. Mater. Chem. 18 (2008) 4510.
[82] J.-D. Cho, J.-W. Hong, Eur. Polym. J. 41 (2005) 367.
[83] V. Sharma, C. Wang, R.G. Lorenzini, R. Ma, Q. Zhu, D.W. Sinkovits, G. Pilania, A.R. Oganov, S. Kumar, G. a Sotzing, S. a Boggs, R. Ramprasad, Nat. Commun. 5 (2014) 4845.
[84] J.-D. Cho, H.-T. Ju, J.-W. Hong, J. Polym. Sci. Part A Polym. Chem. 43 (2005) 658.
[85] J.-D. Cho, J.-W. Hong, J. Appl. Polym. Sci. 93 (2004) 1473.
[86] B.C. Riggs, R. Elupula, S.M. Grayson, D.B. Chrisey, J. Mater. Chem. A (2014).
[87] Y.Q. Li, H.X. Liu, Z.H. Yao, J. Xu, Y.J. Cui, H. Hao, M.H. Cao, Z.Y. Yu, Mater. Sci. Forum 654-656 (2010) 2045.
[88] B.W. Ricketts, I. Physics, G. Triani, A.D. Hilton, N.I. Rd, L. Heights, J. Mater. Sci. Mater. Electron. 11 (2000) 513.
[89] G. Chen, W. Zhang, X. Liu, C. Zhou, J. Electroceramics 27 (2011) 78.
[90] G. Dong, S. Ma, J. Du, J. Cui, Ceram. Int. 35 (2009) 2069.
[91] Q. Wang, L. Zhu, J. Polym. Sci. Part B Polym. Phys. 49 (2011) 1421.
[92] J.J. Li, P. Khanchaitit, K. Han, S.I. Seok, Q. Wang, Abstr. Pap. Am. Chem. Soc. 240 (2010).
[93] Q. Wang, Abstr. Pap. Am. Chem. Soc. 244 (2012).
[94] J.A. Lewis, Curr. Opin. Solid State Mater. Sci. 6 (2002) 245.
[95] A. Kamyshny, M. Ben-Moshe, S. Aviezer, S. Magdassi, Macromol. Rapid Commun. 26 (2005) 281.
[96] H.Y. Ko, J. Park, H. Shin, J. Moon, Chem. Mater. 16 (2004) 4212.
[97] S. Magdassi, A. Bassa, Y. Vinetsky, A. Kamyshny, Chem. Mater. 15 (2003) 2208.
[98] J. Park, J. Moon, Langmuir 22 (2006) 3506.
[99] J. Park, J. Moon, H. Shin, D. Wang, M. Park, J. Colloid Interface Sci. 298 (2006) 713.
[100] B.Y. Tay, J.R.G. Evans, M.J. Edirisinghe, Int. Mater. Rev. 48 (2003) 341.
[101] H.W. Cui, J.T. Jiu, S. Nagao, T. Sugahara, K. Suganuma, H. Uchida, K.A. Schroder, Rsc Adv. 4 (2014) 15914.
[102] Y. Kim, M. Chikamatsu, R. Azumi, T. Saito, N. Minami, Appl. Phys. Express 6 (2013).
[103] G. Cummins, M.P.Y. Desmulliez, Circuit World 38 (2012) 193.
[104] Y. Wu, X. Zhao, F.E.I. Li, Z. Fan, J. Electroceramics 11 (2004) 227.
[105] D. Bergman, Phys. Rep. 9 (1978) 377.
[106] J.Y. Li, L. Zhang, S. Ducharme, Appl. Phys. Lett. 90 (2007) 132901.
[107] I. Webman, J. Jortner, M.H. Cohen, Phys. Rev. B 15 (1977) 5712.
[108] N. Ramakrishnan, P.K. Rajesh, P. Ponnambalam, K. Prakasan, J. Mater. Process. Technol. 169 (2005) 372.
[109] S. Adireddy, V.S. Puli, S.C. Sklare, R. Elupula, T.J. Lou, S.. Grayson, D.B. Chrisey, Flexible Ferroelectric Polymer-NanocrystalComposite Films for Large-Scale Capacitive Energy Storage, Nova Science Publishers, 2014.
[110] S. Adireddy, V.S. Puli, S.C. Sklare, T.J. Lou, B.C. Riggs, R. Elupula, S.M. Grayson, D.B. Chrisey, (2014).
[111] S.H. Liu, J.W. Zhai, Rsc Adv. 4 (2014) 40973.
[112] K. Yu, Y.J. Niu, Y.C. Zhou, Y.Y. Bai, H. Wang, J. Am. Ceram. Soc. 96 (2013) 2519.
[113] L. Gao, J.L. He, J. Hu, Y. Li, J. Phys. Chem. C 118 (2014) 831.
[114] V.S. Puli, R. Elupula, B.C. Riggs, S.M. Grayson, R.S. Katiyar, D.B. Chrisey, Int. J. Nanotechnol. 11 (2014) 910.